

# Modular Multi Target Tracking Using LSTM Networks

Rishabh Verma, R Rajesh and MS Easwaran  
*Centre for Airborne Systems, DRDO*  
*Bengaluru, India -560037*

The process of association and tracking of sensor detections is a key element in providing situational awareness. When the targets in the scenario are dense and exhibit high maneuverability, Multi-Target Tracking (MTT) becomes a challenging task. The conventional techniques to solve such NP-hard combinatorial optimization problem involves multiple complex models and requires tedious tuning of parameters, failing to provide an acceptable performance within the computational constraints. This paper proposes a model free end-to-end approach for airborne target tracking system using sensor measurements, integrating all the key elements of multi target tracking - association, prediction and filtering using deep learning with memory. The challenging task of association is performed using the Bi-Directional Long short-term memory (LSTM) whereas filtering and prediction are done using LSTM models. The proposed modular blocks can be independently trained and used in multitude of tracking applications including non co-operative (e.g., radar) and co-operative sensors (e.g., AIS, IFF, ADS-B). Such modular blocks also enhances the interpretability of the deep learning application. It is shown that performance of the proposed technique outperforms conventional state of the art technique Joint Probabilistic Data Association with Interacting Multiple Model (JPDA-IMM) filter. **Keywords:** Association, Multi-Target Tracking, Bi-directional LSTM, JPDA-IMM, Interpretability.

## I. Introduction

**M**ULTI-TARGET tracking (MTT) in a clutter environment with noisy measurements is a challenging task. A reliable tracking system should be able to accurately estimate the state of the targets, which is often difficult due to the association capabilities and measurement imperfections. Kalman filter (KF) [1] has been a widely used technique for MTT, and many of its variants such as unscented KF (UKF) [2], extended KF (EKF) [3] and particle filter (PF)[4] further improve the tracking accuracy. These techniques require pre-defined mathematical motion models of the targets for tracking and are based on Bayesian tracking theory. However, it is highly unlikely to have precise mathematical models of the targets in advance especially in military scenarios. Since, the performance of such techniques rely on the accuracy of the models, they suffer a serious degradation in the performance due to model imperfections. To improve performance Multiple Model (MM) [5] algorithm uses more than one filters simultaneously to track the target.

Further improvements were made in Interactive Multiple Model (IMM) [6] where the weights of the models are derived according to the changing observations.

A typical MTT process involves association of measurements to tracks, managing birth & death of tracks, prediction of track parameters and filtering of measurements. The process of association in a clutter environment is a NP- hard problem. Many sophisticated algorithms have been developed in the past including the multiple hypothesis tracker (MHT) [7] which generates a tree of potential hypothesis for each target, therefore leads to the combinatorial explosion and computational overload with increase in number of targets. Joint Probabilistic Data Association (JPDA) [8] computes all possible joint events for calculating the association probabilities and requires knowledge of clutter rate and detection probability for computations.

Recently, deep learning based techniques have shown promising results in solving the problem of tracking and association especially in pedestrian tracking [9–11] from videos. Anton Milan et al. [12] used Recurrent Neural Network (RNN) based model for prediction, birth/ death and LSTM based model for association in a two-dimensional (2D) scenario and showed that the neural network without any prior knowledge about target dynamics, clutter distributions etc, is able to perform prediction, data association, and filtering in the context of video tracking. For radar tracking, C.Gao et al. [13] showed that multi layer RNN structures gives better filter results as compared to single layer while both the model outperformed the IMM. Jingxian Liu et al. [14] used Bi-directional LSTM based filtering algorithm in a 2D clutter free environment. Huajun Liu et al. [15] showed LSTM based models performs better association as compared to classic models like JPDA and Hungarian algorithm (HA) in a 2D clutter environment. The papers above only consider parts of MTT problem in the context of sensor measurements and contain targets with low agility and range.

This paper makes the following contributions:

- 1) It considers a 3D scenario with clutter and high maneuvering targets as compared to most of the previous work, that are focused on 2D models and/or clutter free environment.
- 2) It provides an end-to-end model based on deep neural networks for multi-target tracking, consisting- filtering, prediction, track management and association with modular building blocks.
- 3) It uses a Bi-directional LSTM based model for association process and shows that it outperforms LSTM based model in efficient training and performance.
- 4) It provides modular deep learning blocks which can be adopted for MTT problems for both co-operative and non co-operative sensors.
- 5) It characterizes the performance of the end to end approach with conventional approach using Generalized Optimal Sub-Pattern Assignment (GOSPA) [16] metric, showing the effectiveness of the proposed modular blocks.

## II. Multi Target Model

The scenario under consideration has multiple and dense high maneuvering airborne targets. The scenario is sensed by a sensor which induces imperfections modeled as measurement error and false detections originating from clutter. Such a scenario is typical of a large scale military combat.

### A. Motion Model

This paper uses a particle model [17] with three degree of freedom for the aircraft, with the assumption of no slide slip, no angle of attack and no effect of rotation of the earth. The motion of the aircraft with ground coordinate system as inertial frame can be expressed as Eq. (1), where  $x$ ,  $y$ ,  $z$  are the position coordinates of the aircraft,  $v$  is linear velocity,  $\phi_p$  is pitch angle and  $\phi_a$  is azimuth angle of the aircraft. The six dimensional state vector is defined as  $[x, y, z, v, \phi_p, \phi_a]$ .

$$\begin{cases} \dot{x} = v \cos \phi_p \cos \phi_a \\ \dot{y} = v \cos \phi_p \sin \phi_a \\ \dot{z} = v \sin \phi_p \end{cases} \quad (1)$$

The simplified dynamic equations can be described as Eq. (2), where  $n_x$  is normal overload and  $n_z$  is tangential overload. The motion of the aircraft is controlled by the control variables  $[\phi_r, n_z, n_x]$ . The truths are generated by randomly changing the control variables.

$$\begin{cases} \dot{v} = g(n_x - \sin \phi_p) \\ \dot{\phi}_p = \frac{g}{v}(n_z \cos \phi_r - \cos \phi_p) \\ \dot{\phi}_a = \frac{g}{v \cos \phi_p} n_z \sin \phi_r \end{cases} \quad (2)$$

### B. Measurement Model

The measurement model for each measurement the sensor (e.g., radar) outputs matrix  $M = [r, \phi_p^r, \phi_a^r, v_r]$ , where  $r$  is radial distance of target,  $\phi_p^r$ ,  $\phi_a^r$  are pitch and azimuth angles of target and  $v_r$  is radial velocity of the target *w.r.t.* the radar. The four dimensional measurement vector for the sensor is calculated using Eq. (3).

$$M = \begin{bmatrix} \sqrt{x^2 + y^2 + z^2} \\ \tan^{-1}(z/\sqrt{x^2 + y^2}) \\ \tan^{-1}(y/x) \\ \frac{v \cdot r}{|r|} \end{bmatrix} + N \quad (3)$$

Where  $N \sim \mathcal{N}(\mu, \sigma^2)$  is measurement noise added with co-variance matrix  $\sigma^2 = \text{diag}([\sigma_d^2, \sigma_{\phi_p}^2, \sigma_{\phi_a}^2, \sigma_v^2])$ , where  $\sigma_d^2, \sigma_{\phi_p}^2, \sigma_{\phi_a}^2$  and  $\sigma_v^2$  are variance of radial distance, pitch angle, azimuth angle and radial velocity respectively of the target w.r.t. the radar. The above models are used for the generation of truth and measurements for training deep neural networks.

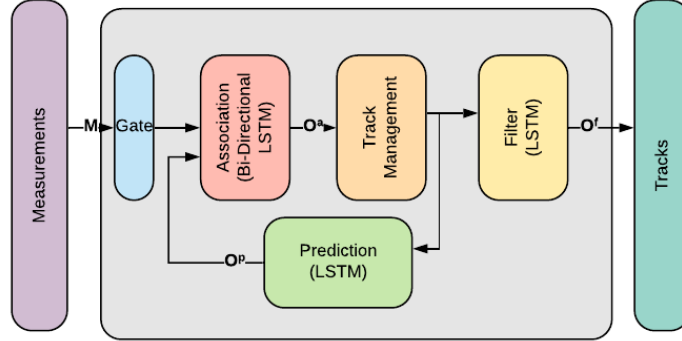


**Fig. 1 Multi Target Tracker**

### III. Deep Learning blocks for Multi-target tracking

The building blocks of the multi-target tracker is shown in Fig. 1. The main blocks are association block which associates a measurement to a track, track management block which takes care of birth and death of the tracks, prediction block which predict the state of the established tracks and filter block which refines the track positions. A gate is used before association block in case when the number of measurements exceed the capacity of association module, it break the measurements into small clusters before feeding to the association module. The gate helps on scaling the algorithm to large number of targets.

The process of prediction and filtering requires the knowledge of both the current and previous states of the aircraft. This task is realized through Long Short-Term Memory (LSTM) [18], which solves the vanishing and exploding gradients problem of RNN using multiple gates. These networks inherently have a memory element which helps in predicting any time series.

Association of a measurement to the correct track requires the knowledge of other tracks and measurements at that instance. This requires a memory element with Bidirectional information flow. Hence, Bi-directional LSTM [19] which initializes two independent LSTMs are used together running in opposite directions capturing both backward and forward information. Track Management implements a birth-death process is implemented using a rate based algorithm.

The measurement matrix  $M$  of dimension  $n \times 4$  where  $n$  is number of measurements, along with matrix  $O^p$  which is output from prediction block and has dimension  $m \times 6$  where  $m$  is the number of established tracks are fed to association block. Association module either associates each track to one of the measurements or NONE, and outputs matrix  $O^a$

with dimension  $(n + 1) \times m$ . The unassociated tracks and measurements go through the track management module, where either the new tracks are formed or the idle tracks are terminated. The filter module refines the measurements for each established tracks and outputs the position, meanwhile the prediction module use measurements to predict the next states of each track and whole cycle repeats.

It can be seen that proposed design is modular and can be used for multiple cooperative and non cooperative sensors. These blocks can be independently tested, integrated together or in parts depending on the sensor of interest.

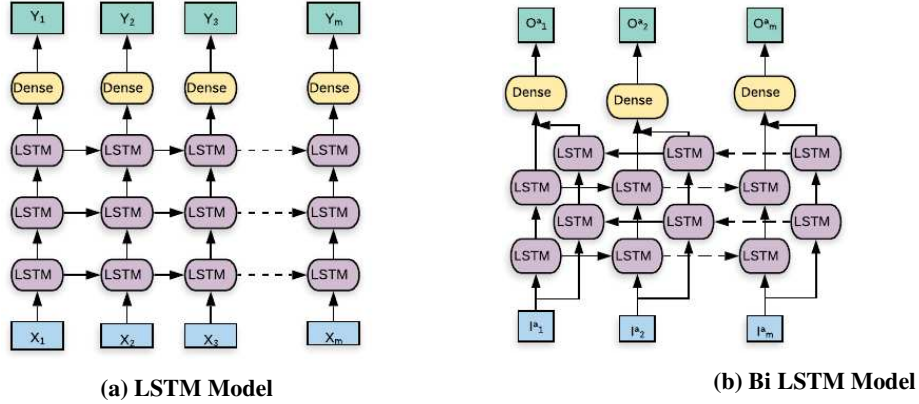


Fig. 2 Deep Learning Models

## IV. Model Free Tracker

### A. Data Generation For Training

Random training tracks are generated with linear velocity  $v$  of targets ranging  $[100, 600]$  m/sec, linear acceleration varying from  $[-2g, 2g]$  and normal acceleration ranging from  $[-2g, 9g]$  according to motion model Eq. (1). Tracks are simulated at interval of 0.1 sec. Radar measurements are generated by sampling the tracks at the interval of 5 sec and adding measurement noise with variance matrix  $\sigma^2 = \text{diag}([\sigma_d^2, \sigma_{\phi_p}^2, \sigma_{\phi_a}^2, \sigma_v^2])$ , where  $\sigma_d^2 = 30m$ ,  $\sigma_{\phi_p}^2$  and  $\sigma_{\phi_a}^2 = 0.5^\circ$  and  $\sigma_v^2 = 5m/s$ . 50,000 random tracks are generated with 100 measurements each, and are divided in training and validation set in 80:20 ratio.

### B. Association

#### 1. Model

Two different models are trained with the same set of training data and compared on the metric of accuracy and training convergence. A two layer Bidirectional LSTM model with hidden layer nodes = 128, and a two layer LSTM model with hidden layer units = 256 as described in Fig. 2b are compared. Loss function used is categorical crossentropy, where for each established track the assignment loss is calculated using Eq. (4), where  $t_i$  is the ground truth and  $s_i$  is the predicted assignment score for the measurement  $i$  to the current track from the sigmoid layer and  $n$

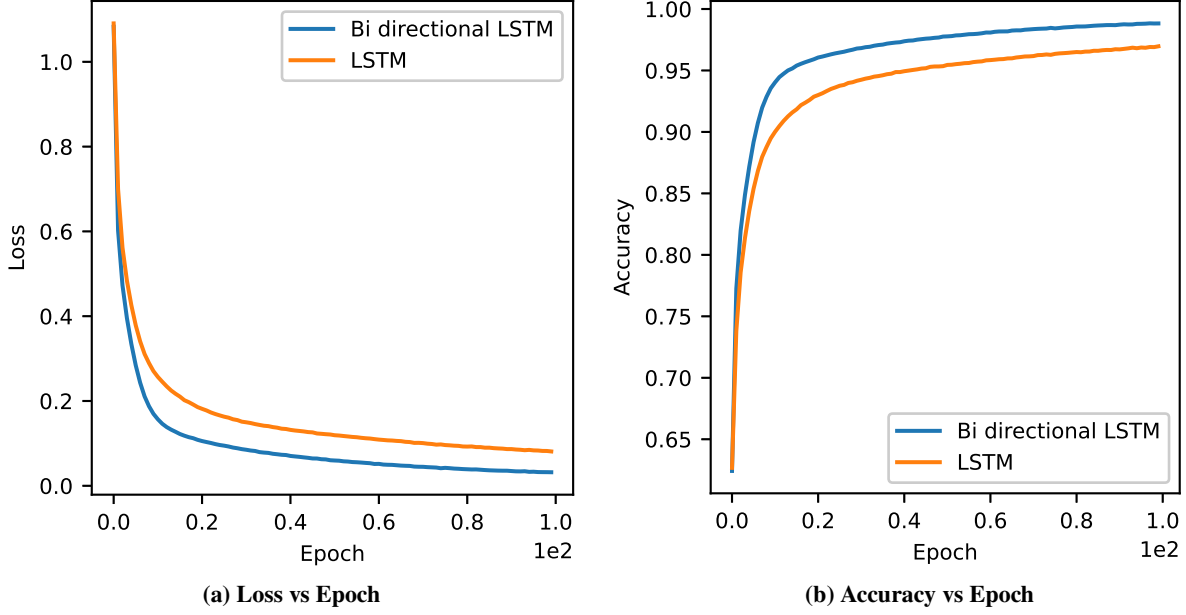


**Fig. 3 Association Model**

is number of measurements.

$$Loss = - \sum_i^n t_i \log(s_i) \quad (4)$$

## 2. Input

The association module at each time step gets input from both radar as matrix  $M$  after gating and prediction module as matrix  $O^p$ , where  $M_l = [r, \phi_p^r, \phi_a^r, v_r]_l$ ,  $l \in [1, n]$ , where  $n$  is the total number of measurements for current time  $t$ . And  $O_k^p = [x, y, z, v_x, v_y, v_z]_k$ ,  $k \in [1, m]$  where  $m$  is number of established tracks.  $I^a$  is  $n \times m$  dimensional matrix, where  $I_k^a$  is  $k^{th}$  input sequence to the model.

$$I_{lk}^a = abs \left( \begin{array}{c} \left[ \begin{array}{c} r * \cos(\phi_p^r) * \cos(\phi_a^r) \\ r * \cos(\phi_p^r) * \sin(\phi_a^r) \\ r * \sin(\phi_p^r) \\ v_r * \cos(\phi_p^r) * \cos(\phi_a^r) \\ v_r * \cos(\phi_p^r) * \sin(\phi_a^r) \\ v_r * \sin(\phi_p^r) \end{array} \right]_l - O_k^p \end{array} \right)$$

### 3. Training

Model is trained for 100 epochs where each epochs contain 10,000 episodes. The total number of dense tracks are chosen randomly between 0 to 10. Model is trained with Adam optimizer[20] with learning rate of 0.001. It can be seen from Fig. 3 that the Bi-directional LSTM outperforms the LSTM in the loss and accuracy metrics with 58.66% and 2.02% respectively.

### 4. Output

The output matrix  $O^a$  of the model is an association matrix, where  $O_{lk}^a \in [0, 1]$  and denotes the likelihood of measurement  $l$  being associated to current track  $k$ , for each track  $k$   $argmax$  is applied to find the associated measurement  $l$ ,  $l \in [0, n]$ , where 0 means unassociated and 1, 2..n are indices of the measurements from the radar.

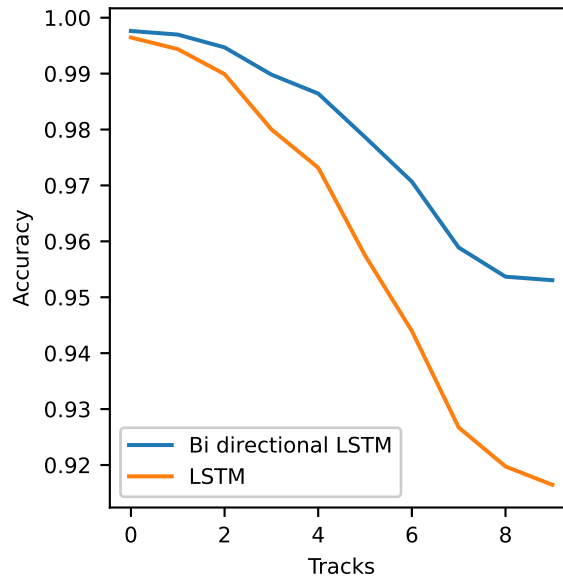


**Fig. 4 Performance on test data**

### 5. Performance

The model is tested on the different scenarios containing crossing tracks ranging from 1 to 8 with motion and measurement model as described in Section II. The measurements also contain false detections. As expected it can be seen in Fig. 4 that the Bi directional LSTM model shows better performance in associating the measurements to the tracks, especially when the number of tracks are higher. Also when the tracks are increased from 1 to 10 there is only 4.41% reduction in accuracy of association.

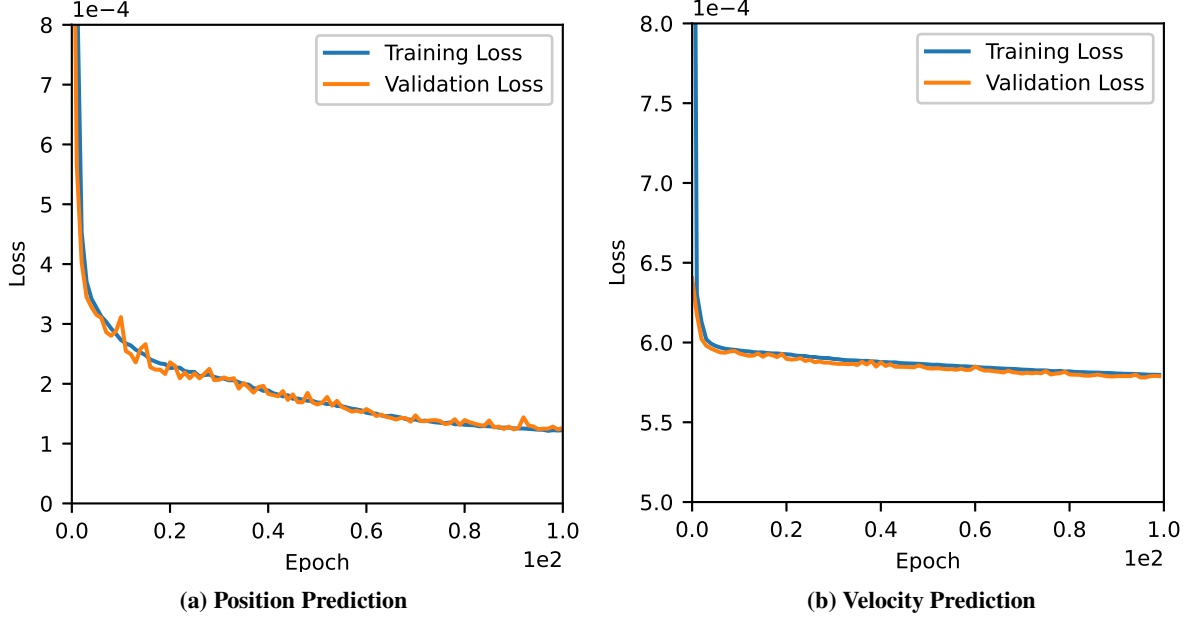


**Fig. 5 Prediction Model**

## C. Prediction Module

### 1. Model

For prediction, two different LSTM based models are used, one for predicting the position coordinates for time  $t + 1$ , and the other for the predicting the radial velocity components along the coordinate axis for time  $t + 1$  from the measurement state at time  $t$ . Both models are identical in shape and training hyper-parameters. A 3 layers stacked LSTM model as described in Fig. 2a with number of nodes in hidden layer = 512 for all layers. Loss function used is Mean Squared Error (MSE), where loss is calculate as Eq. (5), where  $n$  is number of states,  $y_i$  is ground truth of  $i^{th}$  state and  $x_i$  is predicted value.

$$Loss = \frac{1}{n} \sum_{i=1}^n (y_i - x_i)^2. \quad (5)$$

### 2. Input

The input  $I^P$  to the model are the current measurements of the tracks.

$$I_k^P = [x, y, z, v_x, v_y, v_z]_k$$

where  $I_k^P$  is the input for track  $k \in [1, m]$  where  $x, y, z$  are position coordinates and  $v_x, v_y, v_z$  are components of radial velocity *w.r.t.* to coordinate axis and  $m$  is number of current tracks.



### 3. Training

Model is trained on 40,000 tracks with 100 measurements each 5 secs apart with Adam optimizer with learning rate of 0.001. From Fig. 5 it can be seen that the network is not over-fitting and provides good validation loss for both position and velocity prediction.

### 4. Output

The output matrix  $O_k^p$  of the model is input for the association module.

$$O_k^p = [x, y, z, v_x, v_y, v_z]_k$$

$k \in [1, m]$  where  $m$  is number of current tracks,  $x, y, z$  are predicted position coordinates and  $v_x, v_y, v_z$  are components of radial velocity *w.r.t.* to coordinate axis.

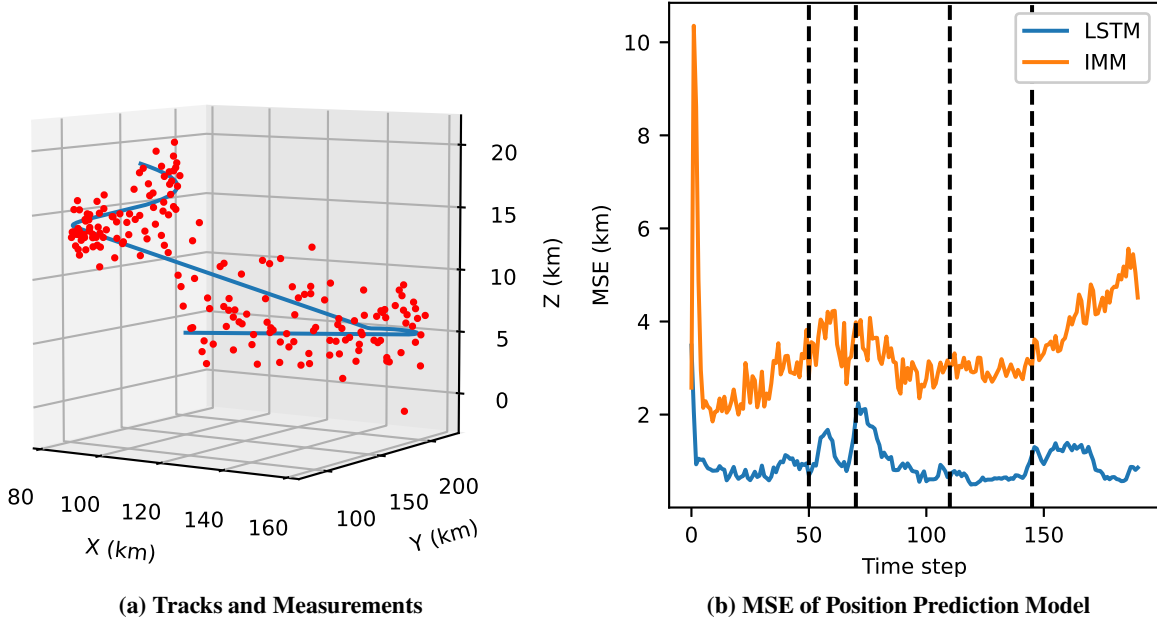


**Fig. 6 Simulation**

### 5. Performance

The model is tested on simulated track shown in Fig. 6a with segments modeled as constant velocity for 50 time steps, coordinated turn for 20 time steps, constant linear acceleration of  $8m/sec^2$  for 35 time steps, constant linear acceleration of  $-8m/sec^2$  for 35 time steps and a spiral turn with linear acceleration of  $5m/sec^2$  for last 50 timesteps. The measurement model is same as described in Section II. The result shown in Fig. 6b is an average Mean Squared Error (MSE) between predicted position and ground truth vs time steps of 100 Monte Carlo runs, with vertical lines marking the switches in motion model. It can be seen that the predictions of LSTM model outperforms the IMM

model in terms of MSE metric and also from figure it is evident that the LSTM model handles the switches between the motion model considerably better than IMM. The overall MSE of predicted positions of LSTM is 71.64% less than the IMM model.

#### D. Filter

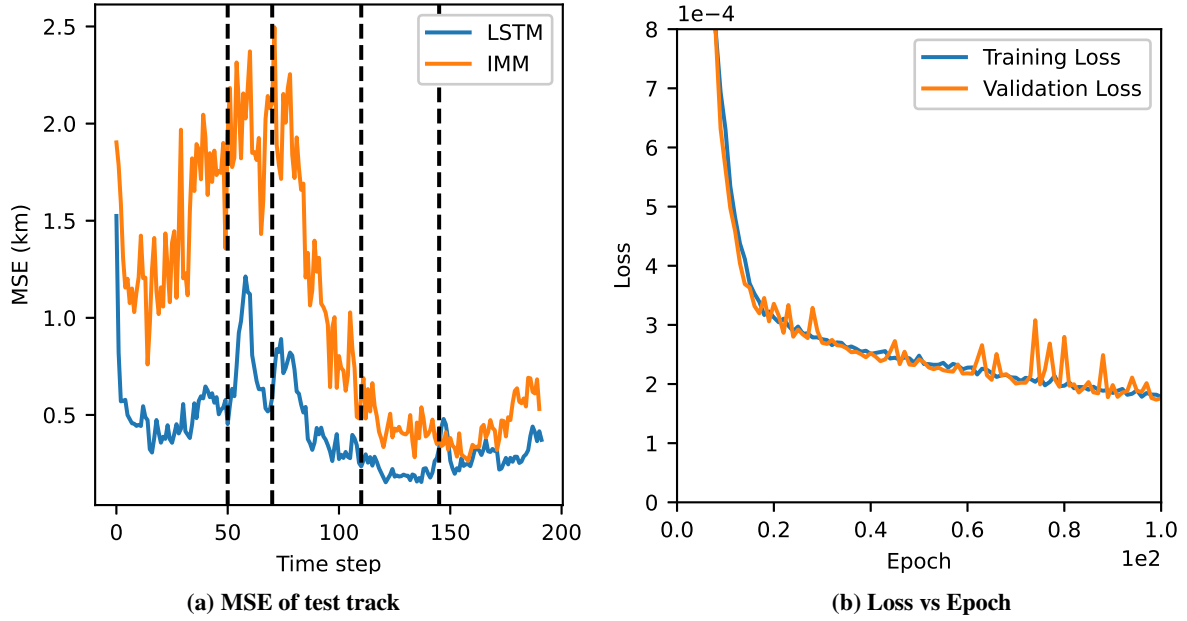


**Fig. 7 Filter Model**

##### 1. Model

In the filter module, a 3 layer LSTM model is used as described in Fig. 2b, with hidden layer nodes = 256 for all layers. Loss function used is Mean Squared Error (MSE), where loss is calculate as Eq. (5), where  $n$  is number of states,  $y_i$  is ground truth of  $i^{th}$  state and  $x_i$  is predicted value.

##### 2. Input

The input  $I^f$  to the model is the associated measurement values, for current time step  $t$ .

$$I_k^f = [x, y, z, v_x, v_y, v_z]_k$$

where  $I_k^f$  is the input for track  $k \in [1, m]$  where  $m$  is number of current tracks  $x, y, z$  are position coordinates and  $v_x, v_y, v_z$  are components of radial velocity *w.r.t.* to coordinate axis.

### 3. Training

Model is trained on 40,000 tracks with sequence length of 100 each 5 secs apart with Adam optimizer with learning rate of 0.001. From Fig. 7b it can be seen that the network gives good validation loss and is not over-fitting.

### 4. Output

The output matrix  $O^f$  of the model is  $O_k^f = [x, y, z]_k$   $k \in [1, m]$  where  $m$  is number of current tracks,  $x, y, z$  are filtered position coordinates.

### 5. Performance

The model is tested on a same simulated track described in Section IV.C.5. Fig. 7a shows the average MSE between filtered position and ground truth vs time steps of 100 Monte Carlo runs. It can be seen that the LSTM model again outperforms the IMM model in filtering and gives 55% better MSE as compared to the IMM.

## E. Track Management

All unassociated measurements  $R$  from the radar goes through an association procedure using gating algorithm in track management module, which maintains a list of probable tracks where the measurement is associated to the track if it falls within the gate of 5 km. Once the total number of measurements of any probable track exceeds the threshold of 5, a new current track  $N$  is formed which from then on wards uses association module for association.

Track management is also responsible to terminate the inactive tracks, if any track is not associated for more than 3 consecutive time steps, it is considered as inactive and is terminated. These numbers are indicative and depend on the target dynamics and sensor characteristic.

## V. Integrated Performance Analysis

The modules described in the paper can be integrated in different ways, based on sensor under consideration. For the specific case of radar all the modules are required. For co-operative sensor like AIS, ADS-B, IFF etc., association module is not required and can be replaced with a conventional "ID" based association engine. Each module can be tuned separately, and can be even replaced by conventional methods. Such a modular system can be tested independently and enhance the interpretability of the overall algorithm.

We use a radar scenario to illustrate the integrated performance. A crossing path scenario as shown in Fig. 8a is used to show the effectiveness of the end-to-end model of this paper. The proposed model is compared with the JPDA-IMM filter on Generalized Optimal Sub-Pattern Assignment metric (GOSPA) [16]. The GOSPA distance is calculated using Eq. (6), where  $X$  and  $Y$  denotes the number of established tracks and ground truth receptively,  $x$  and  $y$  are the estimated position and the ground truth,  $c$  is cutoff distance and  $p$  is the order the metric,  $s$  is switching penalty and  $\eta_s$  is number of switches. GOSPA combines localization errors, errors due to missed targets and false targets, and

also penalizes for track switching.

$$GOSPA = \left( \min_{\pi \in \Pi_{|Y|}} \sum_{i=1}^{|X|} d^{(c)}(x_i, y_{\pi(i)})^p + \frac{c^p}{\alpha} (|Y| - |X|) + s \times \eta_s \right)^{\frac{1}{p}} \quad (6)$$

These are four tracks in the example Fig. 8a. The tracks start with linear velocity of 400 m/sec each and ascend with constant velocity and pitch angle of 0.17 radians for 40 time steps, then all take a coordinated turn with roll angle of 0.26 radians for 15 time steps, and finally accelerate with linear acceleration of  $10 \text{ m/sec}^2$  for next 40 time steps. The vertical lines in Fig. 8b denotes the different motion model segments. The measurement model is same as described in the data generation section with 50 false detections distributed randomly in the space at each time step.

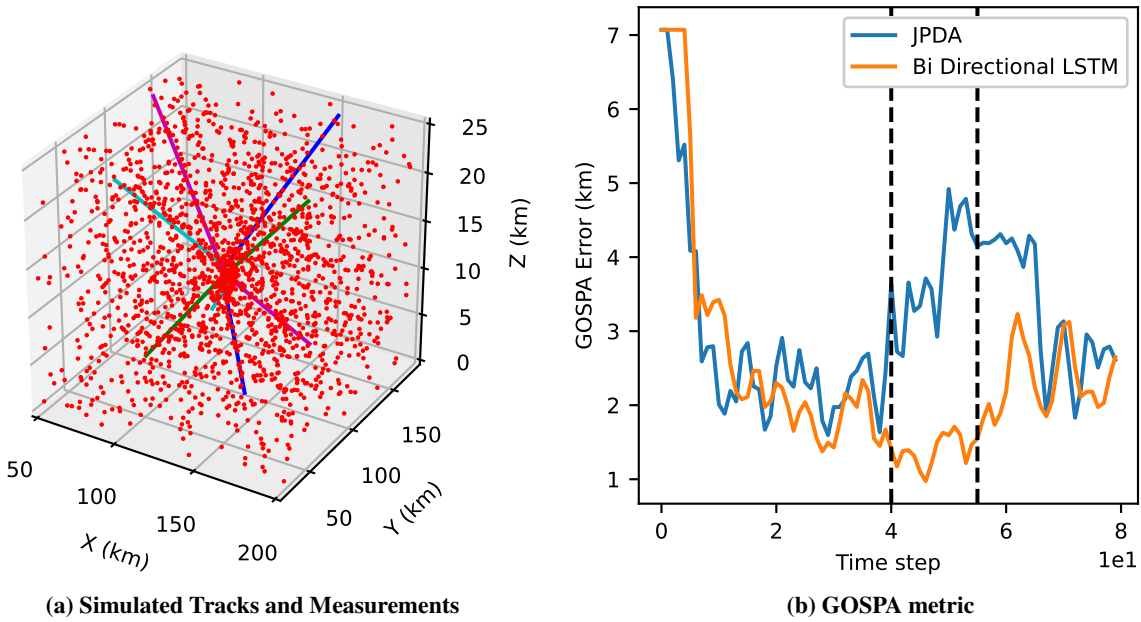


**Fig. 8 Integrated Performance**

The performance of the models are measured in GOSPA with  $p = 2$ ,  $\alpha = 2$ ,  $c = 7$  and  $s = 3$ . Fig. 8b shows the GOSPA distance of both the models w.r.t. time steps. It can be seen that the Integrated LSTM based model performs better as compared to both JPDA especially when tracks converge to the intersection point at  $40^{th}$  time step, it also maintains the track association accuracy and outperforms the JPDA model. The average GOSPA error of proposed integrated algorithm is 25% less than the JPDA-IMM.

## VI. Conclusion

The design and performance of an end-to-end deep learning based modular blocks for multi-target tracking is elucidated in this paper. The modular design provides robustness and easy adaptability towards different measurement sensors and scenarios. The model free approach handles all the process associated with the multi target tracking and

provides better performance to various target motion models encountered in combat than the conventional approaches. The modular design allows fine tuning of specific modules without having to re-train the whole system. The performance of each individual blocks outperforms the conventional state of the art techniques, which is demonstrated using suitable performance metrics. Also, the end to end GOSPA metric of our technique shows good improvement over conventional JPDA-IMM.

## References

- [1] Kalman, R. E., "A New Approach to Linear Filtering and Prediction Problems," *Journal of Basic Engineering*, Vol. 82, No. 1, 1960, pp. 35–45. <https://doi.org/10.1115/1.3662552>.
- [2] Julier, S., Uhlmann, J., and Durrant-Whyte, H. F., "A new method for the nonlinear transformation of means and covariances in filters and estimators," *IEEE Transactions on Automatic Control*, Vol. 45, No. 3, 2000, pp. 477–482. <https://doi.org/10.1109/9.847726>.
- [3] Julier, S. J., and Uhlmann, J. K., "New extension of the Kalman filter to nonlinear systems," *Signal Processing, Sensor Fusion, and Target Recognition VI*, Vol. 3068, edited by I. Kadar, International Society for Optics and Photonics, SPIE, 1997, pp. 182 – 193. <https://doi.org/10.1117/12.280797>.
- [4] Arulampalam, M. S., Maskell, S., Gordon, N., and Clapp, T., "A tutorial on particle filters for online nonlinear/non-Gaussian Bayesian tracking," *IEEE Transactions on Signal Processing*, Vol. 50, No. 2, 2002, pp. 174–188. <https://doi.org/10.1109/78.978374>.
- [5] Xiao-Rong Li, and Bar-Shalom, Y., "Multiple-model estimation with variable structure," *IEEE Transactions on Automatic Control*, Vol. 41, No. 4, 1996, pp. 478–493. <https://doi.org/10.1109/9.489270>.
- [6] Blom, H. A. P., and Bar-Shalom, Y., "The interacting multiple model algorithm for systems with Markovian switching coefficients," *IEEE Transactions on Automatic Control*, Vol. 33, No. 8, 1988, pp. 780–783. <https://doi.org/10.1109/9.1299>.
- [7] Reid, D., "An algorithm for tracking multiple targets," *IEEE Transactions on Automatic Control*, Vol. 24, No. 6, 1979, pp. 843–854. <https://doi.org/10.1109/TAC.1979.1102177>.
- [8] Fortmann, T., Bar-Shalom, Y., and Scheffe, M., "Sonar tracking of multiple targets using joint probabilistic data association," *IEEE Journal of Oceanic Engineering*, Vol. 8, No. 3, 1983, pp. 173–184. <https://doi.org/10.1109/JOE.1983.1145560>.
- [9] Tsai, W. J., Huang, Z. J., and Chung, C. E., "Joint Detection, Re-Identification, And Lstm In Multi-Object Tracking," *2020 IEEE International Conference on Multimedia and Expo (ICME)*, 2020, pp. 1–6. <https://doi.org/10.1109/ICME46284.2020.9102884>.
- [10] Bićanić, B., Oršić, M., Marković, I., Šegvić, S., and Petrović, I., "Pedestrian Tracking by Probabilistic Data Association and Correspondence Embeddings," *2019 22th International Conference on Information Fusion (FUSION)*, 2019, pp. 1–6.

- [11] Babaee, M., Li, Z., and Rigoll, G., “A dual CNN–RNN for multiple people tracking,” *Neurocomputing*, Vol. 368, 2019, pp. 69 – 83. <https://doi.org/https://doi.org/10.1016/j.neucom.2019.08.008>.
- [12] Milan, A., Rezatofighi, S. H., Dick, A., Reid, I., and Schindler, K., “Online Multi-Target Tracking Using Recurrent Neural Networks,” *Proceedings of the Thirty-First AAAI Conference on Artificial Intelligence*, AAAI Press, 2017, p. 4225–4232.
- [13] Gao, C., Liu, H., Zhou, S., Su, H., Chen, B., Yan, J., and Yin, K., “Maneuvering Target Tracking with Recurrent Neural Networks for Radar Application,” *2018 International Conference on Radar (RADAR)*, 2018, pp. 1–5. <https://doi.org/10.1109/RADAR.2018.8557284>.
- [14] Liu, J., Wang, Z., and Xu, M., “DeepMTT: A deep learning maneuvering target-tracking algorithm based on bidirectional LSTM network,” *Information Fusion*, Vol. 53, 2020, pp. 289 – 304. <https://doi.org/https://doi.org/10.1016/j.inffus.2019.06.012>.
- [15] Liu, H., Zhang, H., and Mertz, C., “DeepDA: LSTM-based Deep Data Association Network for Multi-Targets Tracking in Clutter,” *2019 22th International Conference on Information Fusion (FUSION)*, 2019, pp. 1–8.
- [16] Rahmathullah, A. S., García-Fernández, A. F., and Svensson, L., “Generalized optimal sub-pattern assignment metric,” 2017, pp. 1–8. <https://doi.org/10.23919/ICIF.2017.8009645>.
- [17] Zhang, X., Liu, G., Yang, C., and Wu, J., “Research on Air Combat Maneuver Decision-Making Method Based on Reinforcement Learning,” *Electronics*, Vol. 7, No. 11, 2018, p. 279. <https://doi.org/10.3390/electronics7110279>.
- [18] Cho, K., van Merriënboer, B., Gulcehre, C., Bahdanau, D., Bougares, F., Schwenk, H., and Bengio, Y., “Learning Phrase Representations using RNN Encoder–Decoder for Statistical Machine Translation,” *Proceedings of the 2014 Conference on Empirical Methods in Natural Language Processing (EMNLP)*, Association for Computational Linguistics, Doha, Qatar, 2014, pp. 1724–1734. <https://doi.org/https://doi.org/10.3115/v1/D14-1179>.
- [19] Schuster, M., and Paliwal, K. K., “Bidirectional recurrent neural networks,” *IEEE Transactions on Signal Processing*, Vol. 45, No. 11, 1997, pp. 2673–2681. <https://doi.org/10.1109/78.650093>.
- [20] Kingma, D. P., and Ba, J., “Adam: A Method for Stochastic Optimization,” *3rd International Conference on Learning Representations, ICLR 2015, San Diego, CA, USA, May 7-9, 2015, Conference Track Proceedings*, edited by Y. Bengio and Y. LeCun, 2015.